

Learning from Models and Data for Visual Grounding

Ruozhen He¹, Paola Cascante-Bonilla¹, Ziyang Yang¹,
Alexander C. Berg², and Vicente Ordonez¹

¹ Department of Computer Science, Rice University, USA
{catherine.he,pc51,zy47,vicenteor}@rice.edu

² Department of Computer Science, University of California, Irvine, USA
bergac@uci.edu

Abstract. We introduce SynGround, a novel framework that combines data-driven learning and knowledge transfer from various large-scale pre-trained models to enhance the visual grounding capabilities of a pre-trained vision-and-language model. The knowledge transfer from the models initiates the generation of image descriptions through an image description generator. These descriptions serve dual purposes: they act as prompts for synthesizing images through a text-to-image generator, and as queries for synthesizing text, from which phrases are extracted using a large language model. Finally, we leverage an open-vocabulary object detector to generate synthetic bounding boxes for the synthetic images and texts. We finetune a pretrained vision-and-language model on this dataset by optimizing a mask-attention consistency objective that aligns region annotations with gradient-based model explanations. The resulting model improves the grounding capabilities of an off-the-shelf vision-and-language model. Particularly, SynGround improves the pointing game accuracy of ALBEF on the Flickr30k dataset from 79.38% to 87.26%, and on RefCOCO+ Test A from 69.35% to 79.06% and on RefCOCO+ Test B from 53.77% to 63.67%.

Keywords: Visual Grounding · Vision and Language

1 Introduction

Vision-and-language models (VLM) pretrained on image and text pairs have become instrumental across various tasks [30, 40, 42, 60], ranging from object detection [23, 87] to complex visual reasoning [9, 41, 47]. By leveraging web-sourced datasets, these models showcase a strong ability to comprehend and process an extensive vocabulary of objects and scenes, demonstrating remarkable performance even without task-specific tuning.

Among these, the ALBEF model [40] shows a remarkable capability to localize objects in images when using visual explanation methods such as Grad-CAM [72], allowing visual grounding through gradient-based explanations. In addition, existing work has incorporated strategies to improve this grounding

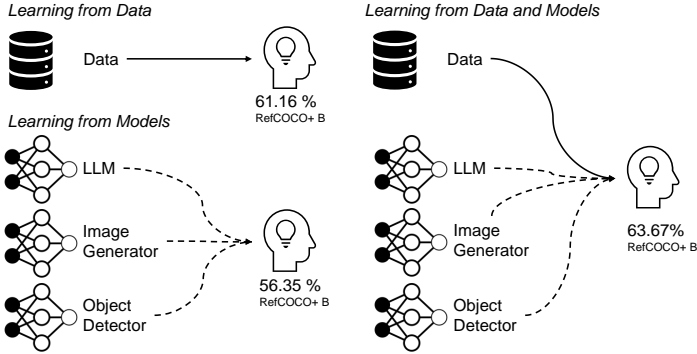


Fig. 1: Data is effective for learning visual grounding, but expensive to curate at scale. In contrast, learning from related models is more flexible yet less effective. Our proposed paradigm leverages the benefits of training using both data and models, improving performance for visual grounding.

capability, finetuning the base model with datasets containing manually curated box annotations [84], or leveraging pretrained object detectors or box proposal networks [9, 18, 24, 31, 43, 84]. The latter circumvents the need for manual annotations, which are particularly expensive to obtain. Our work goes a step further and proposes investigating the potential of using large-scale pretrained models to compensate for the restricted scale of real data by expanding it with affordable synthetic data for visual grounding. This paradigm shift, from *learning from data* to *learning from data and models*, facilitates knowledge transfer across models, leading to higher flexibility and effectiveness in visual grounding (Fig. 1).

Recent advancements in model-based learning focus on generating image-text pairs for image recognition [4, 19, 26, 71, 76, 77]. Learning from generative models has shown promising results when training or tuning representation learners by augmenting real datasets with synthetic data [4], or creating synthetic datasets derived from real data [77]. Some work further improves the *purity* of synthetic data [71, 76] by generating synthetic images based on synthetic captions. However, the synthetic captions used for image synthesis in these studies are generally designed to describe the image as a whole rather than specific regions. These image-level descriptions are usually less effective for visual grounding [27], which instead benefits from object-centric annotations.

In this work, we introduce a pragmatic framework for image-text-box synthesis tailored for visual grounding. To the best of our knowledge, this paper is the first to study to which extent *learning from models* impacts the capability of a pre-trained vision-and-language model to localize objects in an image given a visual explanation. We navigate from lower to higher synthetic purity levels, and break down our investigation of synthetic image-text-box generation into image-text pairs and image-text-box synthesis. Our method, SynGround, leverages a captioning model to generate dense textual descriptions, used for image synthesis. The generated image descriptions are fed into an LLM for text synthesis. Finally, the image-text-box generation is complemented with synthetic

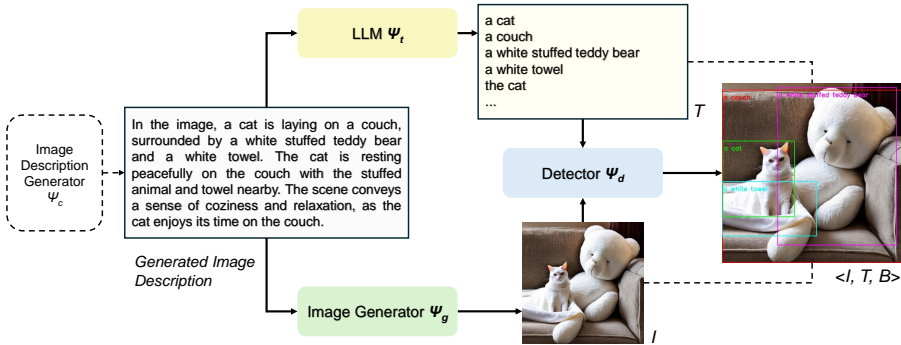


Fig. 2: Overview of our image-text-box synthesis pipeline. We use an image description generator Ψ_c , which outputs a description that serves as a prompt to an image generator Ψ_g to obtain synthetic image I . We also use this description to obtain text phrases T by prompting an LLM Ψ_t . Finally, we input the synthetic text and image into an object detector Ψ_d to obtain synthetic boxes B .

bounding boxes from an open-vocabulary object detector. Remarkably, finetuning a base pretrained vision-and-language model on such synthetic set leads to a substantial performance gain, showcasing the potential of learning from models. More importantly, it reaches new heights when learning from models and data by finetuning on both real and synthetic data.

Our key contributions are summarized as follows.

- We propose a learning from models and data paradigm for visual grounding through image-text-box synthesis, utilizing exhaustive image descriptions for image synthesis, an LLM for text synthesis from phrase extraction, and an open-vocabulary object detector for bounding box generation.
- We investigate a feasible way to generate expandable and effective synthetic image-text-boxes at a higher synthetic purity level.
- We show the effectiveness of our method by outperforming a model exclusively learned from data, contributing to 7.88% improvement on Flickr30k, 9.71% and 9.90% improvement on RefCOCO+ Test A and B, respectively.

2 Related Work

2.1 Visual Grounding

Visual grounding associates textual descriptions with relevant regions within images. Supervised methods are typically trained with image-text-box pairs [14, 15, 18, 32, 84], or integrate pretrained object detectors [25, 62] to identify the most relevant regions with the textual descriptions [9, 13, 21, 24, 48, 81]. While weakly-supervised methods eschew the need for bounding boxes [3, 27, 73, 74], they rely on datasets such as Visual Genome [36], which provide multiple phrases describing various regions in each image. However, the process of manually annotating dense textual descriptions and their corresponding bounding boxes is time-consuming and labor-intensive.

Related to grounding approaches incorporating visual explanation tuning [27, 40, 82, 84], we explore visual grounding in a generalized context, aiming to localize phrases using gradient-based model explanations rather than generating bounding boxes [42]. We leverage GradCAM [72], a heatmap that denotes spatial relevance, to pinpoint phrases within images. Compared to boxes, heatmap provides a more flexible representation for general grounding, especially for visual content that is not easily encapsulated by boxes, such as scenarios involving multiple objects. The state-of-the-art method AMC [84] proposes an attention mask consistency objective to optimize the gradient-based explanations of base-model ALBEF [40] to improve localization performance. Similarly, we adopt ALBEF as our base model and tune it with AMC objectives on image-text-box pairs, employing a gradient-based strategy. This paper delves into the efficacy of synthetic image-text-box in a general visual grounding setting.

2.2 Learning from Synthetic Data

The utilization of synthetic data has been widely explored across various computer vision tasks, including image classification [20, 52, 58], semantic segmentation [10, 63, 65], object detection [57, 68], human pose estimation [34, 80], action recognition [79], autonomous driving [1], and many other domains [12, 28, 37, 50, 51, 53, 66, 67, 78, 83, 85]. In contrast to works that derive synthetic data from 3D-rendered datasets [22, 88] utilizing physically realistic engines [6, 7, 17, 20, 49], our approach aligns more closely with research adopting open-source diffusion models. He *et al.* [26] use GLIDE [54] generated synthetic images to improve pretrained CLIP [60] in zero-shot and few-shot classification, while its performance is adversely affected when trained from scratch on synthetic data. Azizi *et al.* [4] fine-tune Imagen [70] on ImageNet [69] and subsequently leverage its synthetic data to augment the real ImageNet training set, resulting in initial improvement followed by degradation upon scaling up. Fan *et al.* [19] investigate the scaling laws of synthetic images and identify related factors. StableRep [77] propose a self-supervised method with a multi-positive contrastive loss that learns representations from synthetic images generated for captions in large-scale datasets [8, 16], thereby boosting linear probing image classification performance. SynCLR [76] further advances the synthetic level by utilizing LLM-generated synthetic captions. Our research not only generates image-text pairs but also provides corresponding synthetic boxes, facilitating a comprehensive exploration of the efficacy of synthetic image-text-box triplets in visual grounding.

3 Method

This paper studies generating effective synthetic image-text-boxes $\langle I, T, B \rangle$ to improve the visual grounding ability of a base vision-and-language model. The base model consists of a text encoder ϕ_t , a visual encoder ϕ_v , and a multimodal fusion encoder ϕ_f . Section 3.1 introduces the objectives that tune the base model on image-text pairs $\langle I, T \rangle$ and image-text-box triplets $\langle I, T, B \rangle$. Section 3.2 introduces the first step in the synthesis process that uses an image description generator Ψ_c to generate input captions. Section 3.3 introduces image-text synthesis

with an image generation model Ψ_g and a large language model Ψ_t . Section 3.4 describes box synthesis through an object detector Ψ_d .

3.1 Visual Grounding Objectives: Preliminaries

Vision-language Objectives. We adopt ALBEF [40] as the base model, incorporating vision-language objectives including a standard image-text matching loss (\mathcal{L}_{itm}), an image-text contrastive loss (\mathcal{L}_{itc}) and a masking language modeling loss (\mathcal{L}_{mlm}). The image-text matching loss (\mathcal{L}_{itm}) evaluates the compatibility between an image and a text by analyzing the output of [CLS] tokens. Essentially, this loss measures how well the model can predict whether a given image and text pair match, using a cross-entropy loss between the prediction and a one-hot vector indicating whether an image-text pair $\langle I, T \rangle$ match. Next, the image-text contrastive loss (\mathcal{L}_{itc}) is designed to fine-tune the alignment between visual and textual representations. It exploits contrastive learning with a set of negative samples and a temperature scaling parameter to normalize the scores. Finally, the masking language modeling loss (\mathcal{L}_{mlm}) uses both visual inputs and textual context to predict masked tokens from the masked input text. The overall vision-language objective to tune the base model on image-text pairs for representation learning is $\mathcal{L}_{vl} = \mathcal{L}_{itm} + \mathcal{L}_{itc} + \mathcal{L}_{mlm}$.

Attention Map Consistency Objective. Additionally, we leverage an attention map consistency objective which was recently proposed by Yang *et al.* [84] to add box supervision. This objective leverages gradient-based explanation maps (heatmap) G by calculating the gradient of the intermediate feature map in a multimodal fusion encoder ϕ_f and maximizes the consistency between this map and region annotations. This objective considers two terms. The first term \mathcal{L}_{max} encourages the maximum value of the heatmap G inside the target box B to surpass the maximum value outside by a margin δ_1 .

$$\mathcal{L}_{max} = \mathbb{E}_{(I,T,B) \sim D} \left[\max(0, \max_{i,j} ((1 - B_{i,j}) G_{i,j}) - \max_{i,j} (B_{i,j} G_{i,j}) + \delta_1) \right], \quad (1)$$

where $B_{i,j}$ is 1 when the pixel location i, j is inside the box, and zero otherwise. The second term \mathcal{L}_{mean} encourages the mean value of the heatmap G inside the box to be larger than the mean value outside by a margin δ_2 .

$$\mathcal{L}_{mean} = \mathbb{E}_{(I,T,B) \sim D} \left[\max(0, \frac{\sum_{i,j} (1 - B_{i,j}) G_{i,j}}{\sum_{i,j} (1 - B_{i,j})} - \frac{\sum_{i,j} B_{i,j} G_{i,j}}{\sum_{i,j} (B_{i,j})} + \delta_2) \right]. \quad (2)$$

The full \mathcal{L}_{amc} objective is $\mathcal{L}_{amc} = \lambda_1 \cdot \mathcal{L}_{max} + \lambda_2 \cdot \mathcal{L}_{mean}$, where λ_1, λ_2 are trade-off hyperparameters. The base model is tuned with both the \mathcal{L}_{vl} and \mathcal{L}_{amc} objectives.

3.2 Generating Input Captions

Our image-text-box synthesis process initiates with an image description generator Ψ_c , aiming to generate text conditions for image synthesis and queries for text

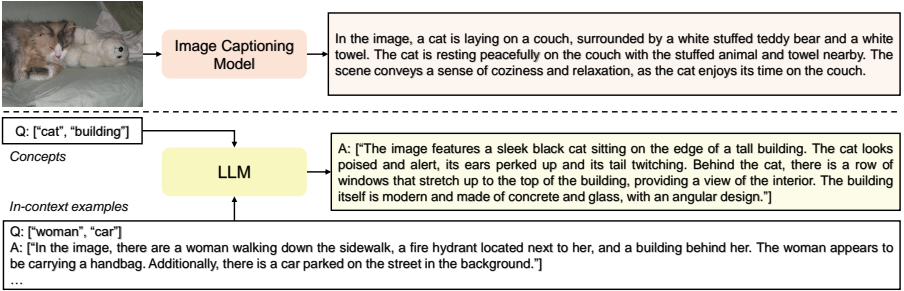


Fig. 3: Two approaches for generating image descriptions (Ψ_C) to use for image synthesis and from which to extract phrases. The top pipeline relies more on real data, applying an image captioning model to real images. The bottom pipeline samples concepts from a predefined list and uses an LLM with in-context learning to generate image descriptions.

synthesis. As shown in Fig. 3, we consider two strategies for image description generation. The first strategy, *Image2Text*, applies an image captioning model on a real image I^R prompted to obtain detailed descriptions. The second strategy, *Concept2Text*, starts with concept sampling from a predefined concept list and an in-context learning example database of detailed captions. The concept list is collected from the real text T^R , while the in-context-learning example database is built through image captioning on a small subset of real images I^R . This second strategy relies less on real data by using the in-context learning ability of an LLM Ψ_t which is used to generate more captions.

3.3 Generating Text and Images

This section explores a crucial aspect of image-text-box synthesis: generating effective image-text pairs tailored for visual grounding. To investigate a model-based paradigm in visual grounding, we first delve into an approach to synthesize image-text pairs that are not only aligned but also inherently equipped for visual grounding. As illustrated in Fig. 4, we investigate three distinct alternatives for conditioning a text-to-image generation model Ψ_g .

The first strategy, *Concatenation*, involves merging all captions associated with a real image I , using this concatenated text as a prompt for text-to-image generation model Ψ_g . Given common restrictions on the number of input tokens for the input text prompt [60] in Ψ_g , we propose a second strategy, *Text2Text*, by drafting a succinct summary through an LLM Ψ_t . In contrast to the strategies above that derive text prompts from existing textual content, we also consider an alternative, *Image2Text*, that employs an image captioning model Ψ_c to generate new captions for real images I^R as input prompts for Ψ_g .

3.4 Generating Boxes

Building upon image-text synthesis, this section supplements the paradigm for image-text-box synthesis (See Fig. 2). It further translates input captions for

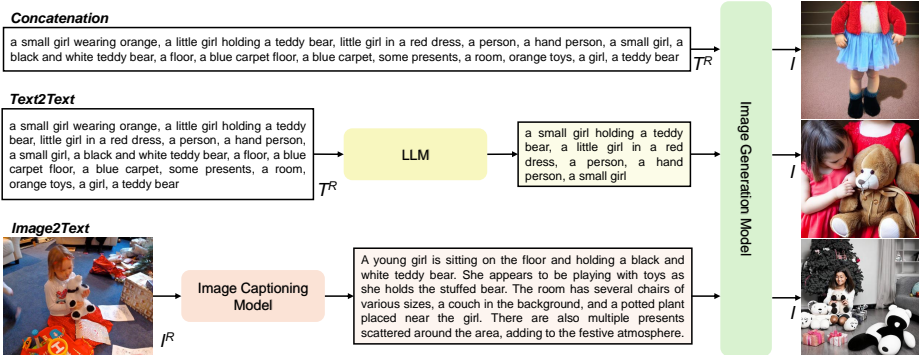


Fig. 4: Illustration of various approaches for image and image description synthesis. Image descriptions can be generated by concatenating real text T^R , LLM summary on real text T^R , and image captioning on real image I^R . Synthetic images I are obtained through an image generator model conditioned on image descriptions.

generating images I to synthetic text phrases T suitable for visual grounding, and facilitates the synthesis of corresponding bounding boxes B . To convert a detailed description paragraph from the image captioning model into a series of region-specific phrases conducive to visual grounding, we prompt the LLM Ψ_t with four manually crafted in-context learning examples for phrase extraction. Following phrase extraction, we exploit a large-scale pretrained open-vocabulary object detector Ψ_d , to generate bounding boxes B for each extracted phrase T . With this process, we synthesize image-text-box triplets $\langle I, T, B \rangle$.

4 Experiments

4.1 Implementation Details

Image-Text-Box Synthesis. To favor reproducibility and accessibility, we adopt Stable Diffusion 2.1 [64] with guidance scale 10.0 as the text-to-image generator Ψ_g , an open-source LLM Vicuna-13B [11] as Ψ_t , and GLIP [42] as the object detector Ψ_d . We select the box with top-1 confidence if it is greater than the default confidence threshold (0.7) in the official implementation. For image description generation Ψ_c , we experiment with BLIP-2 [38] and LLaVA [46] for the *Image2Text* strategy. For the *Concept2Text* variant, we use Vicuna-13B [11] to generate image descriptions from a two-concept query with four randomly sampled in-context examples. The concept list contains nouns extracted from real VG captions. The in-context learning example database encompasses 500 randomly sampled LLaVA-generated image captions.

Visual Grounding Tuning. We employ ALBEF-14M [40] as our base model for its reported visual grounding performance through GradCAM [72]. ALBEF is pretrained on image-text pairs from Conceptual Captions [8], ImageNet-1k [69], MS-COCO [45], SBU Captions [56] and Visual Genome [36]. Tuning for visual grounding applies \mathcal{L}_{v1} on image-text pairs and a combination of \mathcal{L}_{v1} and \mathcal{L}_{amc} on

Table 1: Learning from data and models. We compare the visual grounding improvements for the off-the-shelf base model (row 1) by learning from the real data (row 2), models (row 3), and both (row 4).

Method	Source	Num.	RefCOCO+		Flickr30k	Δ_{avg}
			Test A	Test B		
ALBEF [40]	Off-the-Shelf	-	69.35	53.77	79.38	-
AMC [84]	Data	1,649,546	78.89	61.16	86.46	+8.00
SynGround _M	Models	998,406	73.70	56.35	86.89	+4.81
SynGround	Data&Models	2,627,952	79.06	63.67	87.26	+9.16

image-text-box triplets, adhering to the coefficient settings $\delta_1 = 0.5$, $\delta_2 = 0.1$, $\lambda_1 = 0.8$, and $\lambda_2 = 0.2$ as originally proposed in Yang *et al.* [84].

The training is conducted on a single node with 8 NVIDIA A40 GPUs. Input images undergo resizing to 256×256 pixels and benefit from a suite of augmentations, including color jittering, horizontal flipping, and random grayscale conversion. All experiments use an Adam optimizer [35] with a learning rate set to $1e-5$ and a batch size of 512.

Visual Grounding Evaluation. Following prior works [2, 40, 84], our evaluation uses pointing game accuracy, which measures the proportion of instances where the maximal activation point within the generated heatmaps correctly falls within the annotated ground-truth bounding box regions. We utilize pointing game accuracy as a metric across several benchmark datasets, including RefCOCO+ [86] and Flickr30k [59].

4.2 Learning from Models and Data

Table 1 presents comparisons among learning exclusively from data, from models, and a combination of both. The baseline performance (row 1) is significantly enhanced by incorporating synthetic data generated through model-based learning, yielding an average improvement of 4.81% (row 3). While it falls short of the gains achieved through learning from data (row 2), our proposed method, SynGround, excels by integrating both sources, resulting in an average improvement of 9.16%. SynGround outperforms the state-of-the-art AMC [84] on RefCOCO+ [86] Test A and B, and Flickr30k [59] benchmarks.

4.3 Synthetic Image-Text Pairs with Vision-language Objectives

In this section, we compare the effectiveness of various synthetic image-text synthesis strategies on visual grounding performance. Considering the generation of regional phrases and images containing multiple objects as key steps toward image-text-box synthesis, we tune our base model on synthetic image-text pairs using vision-language objectives. Although the vision-language objectives are not

Table 2: Comparisons of image and text synthesis strategies. We assess the effectiveness of synthetic image-text pairs from text concatenation, Text2Text, and Image2Text pipelines, by evaluating the performance change of tuning a base model.

Category	Image	Text	Num.	RefCOCO+		Flickr30k	Δ_{avg}
				Test A	Test B		
Off-the-Shelf	-	-	-	69.35	53.77	79.38	-
Real	VG	VG	1,649,546	71.41	54.06	79.90	+0.96
Concatenation	Syn-C	VG	1,649,546	67.57	53.14	76.99	-1.60
Text2Text	Syn-V	VG	1,649,546	67.41	52.14	77.80	-1.72
	Syn-V	LLM _C	530,233	70.28	52.08	78.97	-0.39
Image2Text	Syn-B	VG	1,649,546	56.88	48.48	73.93	-7.74
	Syn-B	BLIP-2 _C	267,199	68.15	51.50	78.30	-1.52
	Syn-L	VG	1,649,546	65.35	50.28	76.85	-3.34
	Syn-L	LLaVA _P	384,455	70.22	52.30	78.34	-0.55
	Syn-L	LLaVA _C	716,198	69.94	53.26	78.83	-0.16
	Syn-L	LLaVA _L	680,093	69.84	53.61	79.44	+0.13
	Syn-L	LLaVA _S	1,031,521	70.31	52.55	80.73	+0.36

designed specifically for visual grounding, we notice that well-aligned regional phrases with images containing rich content from VG can improve the visual grounding performance by 0.96% on average (Table 2, row 2).

Table 2 presents a comparative analysis of three synthetic image-text generation strategies: *Concatenation*, *Text2Text*, and *Image2Text*, as outlined in Section 3.3. By concatenating all VG captions to synthesize images (Syn-C), the concatenation strategy degrades the average grounding performance by 1.60%. It indicates that our text-to-image generation model Ψ_g fails to generate all visual content from the long yet potentially redundant prompts. To shorten the prompt, we utilize an LLM Ψ_t to summarize attributes for the same objects. The 4th row shows the misalignment between the *Text2Text* synthetic image (Syn-V) and the original VG captions. The 5th row shows that tuning the model on Syn-V and object-centric phrases from splitting the LLM summary by comma (LLM_C) is not effective.

As for the *Image2Text* strategy, we experiment with two distinct styles of image captioning models: BLIP-2 [38] that yields condensed phrases, and LLaVA [46] that produces detailed paragraphs. Both BLIP-2 and LLaVA prompted images (Syn-B and Syn-L, respectively), when paired with original VG captions (rows 6 and 8) show that the information between the manually crafted texts and model-generated texts does not completely overlap. Notably, an opposite influence is observed when Syn-B and Syn-L are paired with phrases extracted from their generated image captions. Since BLIP-2 generated captions usually include short object-centric phrases (*e.g.* "a dog, a cat"), we convert the captions into phrases

(BLIP-2_C) for visual grounding through comma separation. Although compared to the Syn-B and VG caption result (row 6), using BLIP-2_C leads to better performance, possibly due to better cross-modal alignment, it is still below the baseline.

Conversely, images synthesized via LLaVA (Syn-L) and paired with phrases extracted from LLaVA captions can enhance grounding performance (rows 11 and 12), indicating that detailed prompts are better suited to the text-to-image synthesis model. We compare four ways to partition the LLaVA captions into phrases: LLaVA_P and LLaVA_C, segmented by periods and commas, respectively, while LLaVA_L for longer LLM extracted phrases and LLaVA_S for shorter phrases. Our experiments demonstrate that the Image2Text strategy, particularly when integrating the LLaVA captioner and LLM for phrase extraction, yields the most effective synthetic image-text pairs for visual grounding.

4.4 Synthetic Image-Text-Boxes with AMC Objectives

In this section, we discuss two pipelines for image-text-box synthesis as detailed in Table 3. The first involves an open vocabulary object detector GLIP [42] to generate regional annotations for each synthetic text phrase (see Fig. 3), building upon the success of *Image2Text* in Section 4.3. For this pipeline, we compare pairing the synthetic images with shorter phrases (LLaVA_S), longer phrases (LLaVA_L), and both (LLaVA_{S,L}). The shorter phrases outperform others (row 3), leading to an average performance gain of 4.81% (row 3). However, merging shorter and longer phrases (LLaVA_{S,L}) –despite increasing the amount of data– does not further improve performance, suggesting redundancy in the information conveyed by the different phrase lengths.

Our alternative strategy leverages the layout-conditioned generative model GLIGEN [44], synthesizing images conditioned on the text and corresponding bounding boxes. Directly inputting all real VG texts and boxes (row 6) results in a modest increase of 2.58% compared to the baseline (row 1). We observe the ineffectiveness in regions with multiple textual descriptions, tending to generate unrealistic or implausible visual content. To address it, we explore three strategies: Random selection of text-box inputs (Random), reduction based on average CLIP [60] text dissimilarity (Text), and the largest collection of boxes with IoU below 0.5. The random selection keeps at most 10 boxes per image, resulting in around 50% data amount reduction. The Random text-box synthesized images Syn-R (row 8) outperforms the all-text-box conditioned variant (Syn-A, row 6). Also, pairing Syn-R with all text-box data from Real VG (row 7) does not match the effectiveness of either Syn-A with all text-boxes or Syn-R with selected text-boxes, underscoring the importance of image-text-box alignment. Sorting by CLIP text dissimilarity to select at most top-10 inputs (Syn-T) marginally improves the random selection. Yet, the most significant improvement stems from selecting as many boxes as possible with an IoU below 0.5. The images (Syn-I) generated with this strategy match the best practice in the GLIP-based pipeline (row 3).

Our results show the potential of using a layout-conditioned generative model for image-text-box synthesis. However, either generating non-overlapping and

Table 3: Effectiveness of synthetic image-text-boxes generated from two strategies. The GLIP strategy involves obtaining boxes through an object detector on synthetic images, while GLIGEN represents generating images conditioned on text and boxes.

Category	Image	Text	Num.	RefCOCO+		Flickr30k	Δ_{avg}
				Test A	Test B		
Off-the-Shelf	-	-	-	69.35	53.77	79.38	-
Real	VG	VG	1,649,546	78.89	61.16	86.46	+8.00
GLIP	Syn-L	LLaVA _S	998,406	73.70	56.35	86.89	+4.81
	Syn-L	LLaVA _L	659,927	72.39	55.94	86.53	+4.12
	Syn-L	LLaVA _{S,L}	1,658,333	72.25	57.05	86.71	+4.50
GLIGEN	Syn-A	VG	1,649,546	68.79	56.88	84.57	+2.58
	Syn-R	VG	1,649,546	68.25	55.78	84.59	+2.04
	Syn-R	Random	725,974	71.66	56.15	84.84	+3.38
	Syn-T	Text	725,974	71.80	56.68	84.73	+3.57
	Syn-I	IoU	652,657	73.05	58.38	84.39	+4.44

natural layouts or generating text for visually coherent layouts poses a substantial challenge, limiting the advancement to a higher synthetic purity level without real image-text-box data. Even with layout generation models [29, 33], strong constraints of natural composition and non-overlapping bounding boxes detract from their efficiency and effectiveness compared to the object detector approach.

4.5 Feasibility of Using Higher Synthetic Purity

In this section, we investigate the feasibility of synthesizing image-text-boxes at a higher level of synthetic purity, aiming to achieve comparable performance with our lower-purity counterparts. Purity refers here to how much do we rely on real data in the prompting of various models in order to generate synthetic data. SynGround^H achieves a higher level of synthetic purity by incorporating the image description generator that relies less on real data. It substitutes real images and the image captioning model with an extracted concept list, an in-context learning example database, and an LLM (see Fig. 3). As shown in Table 8, this higher synthetic purity strategy (SynGround_M^H, SynGround^H) not only rivals but matches the performance of the lower synthetic purity variant on benchmarks. This includes scenarios where learning exclusively from models (rows 3, 4) as well as learning from both data and models (rows 5, 6). It indicates the potential of learning from data and models in a more scalable and flexible setting.

4.6 Factors Causing the Performance Gap with the Real Data

Table 5 analyzes the factors contributing to the performance gap between synthetic and real data. Experiment I is the off-the-shelf ALBEF performance, serv-

Table 4: Performance comparisons with pipelines at different synthetic purity levels due to different image description generators. SynGround_M and SynGround are of lower purity for relying on real images, whereas SynGround_M^H and SynGround^H achieve higher purity through the utilization of a concept list and in-context examples.

Method	Source	Num.	RefCOCO+		Flickr30k	Δ_{avg}
			Test A	Test B		
ALBEF [40]	Off-the-Shelf	-	69.35	53.77	79.38	-
AMC [84]	Data	1,649,546	78.89	61.16	86.46	+8.00
SynGround _M	Models	998,406	73.70	56.35	86.89	+4.81
SynGround _M ^H	Models	979,861	72.18	55.92	86.30	+3.97
SynGround	Data&Models	2,627,952	79.06	63.67	87.26	+9.16
SynGround ^H	Data&Models	2,629,407	79.10	62.94	86.93	+8.82

ing as a baseline. In experiment II, we provide the results from training on real VG image-text-boxes, leading to an average improvement of 8%. Experiment III retains real images and texts from VG, but employs GLIP-generated boxes. The 1.02% decrease in performance compared to experiment II suggests that the synthetic boxes, while effective, may lack the precision of hand-annotated equivalents. Experiment IV further replaces the real VG captions with synthetic ones from SynGround (*i.e.* LLaVA_S), resulting in an additional average reduction of 1.83%. This decline could stem from a reduction in the number of captions (~600K fewer) or discrepancies in visual-textual alignment, coverage, and diversity compared to manually curated captions. Intriguingly, the performance on Flickr30k is enhanced by 1.03% over the real data setting (II), showing a potential distribution shift from synthetic captions. In experiment V, the paradigm shifts entirely to synthetic image-text-box data, eliminating real images from the dataset. Compared to IV, it modestly drops another 0.34%. This minor decrement, relative to the changes observed with synthetic texts and boxes, indicates that synthetic images maintain a level of effectiveness for visual grounding tasks comparable to their real counterparts.

4.7 Alternative Paradigm Design

Table 6 compares two strategies of distinct sequence on phrase extraction (See Fig. 5). The "Caption" strategy adopted in SynGround obtains the synthetic phrases for visual grounding by applying LLM phrase extraction on captions derived from captioning the real VG images (row 2). Alternatively, "ReCaption" extracts phrases from paragraphs captioned on synthetic images. The core comparison between the "Caption" and "ReCaption" paradigms essentially boils down to evaluating the visual-textual misalignment introduced by image synthesis via a text-to-image model ("Caption") against the misalignment from an

Table 5: Factors causing the performance gap with the real data. We investigate how each model caused the ineffectiveness compared to the real data. I is the off-the-shelf performance of our base model. II is learning from real data. From III to V, we sequentially replace the real box, text, and image with synthetic variants.

Exp.	Image	Text	Box	Num.	RefCOCO+		Flickr30k	Δ_{avg}
					Test A	Test B		
I	-	-	-	-	69.35	53.77	79.38	-
II	VG	VG	VG	1,649,546	78.89	61.16	86.46	+8.00
III	VG	VG	GLIP	1,599,633	76.88	59.79	86.76	+6.98
IV	VG	LLaVA _S	GLIP	1,000,634	73.11	57.35	87.49	+5.15
V	Syn-L	LLaVA _S	GLIP	998,406	73.70	56.35	86.89	+4.81

image captioning model ("ReCaption"). Table. 6 reveals a consistent observation with Table 5 that information loss or misalignment stems from the text synthesis, specifically image captioning on synthetic images in this experiment, rather than the image synthesis.

Table 6: Data synthesis comparisons. "ReCaption" denotes applying an image captioning model to synthetic images, whereas "Caption" is applied on real images.

Paradigm	RefCOCO+		Flickr30k
	Test A	Test B	
ReCaption	73.09	56.33	86.80
Caption	73.70	56.35	86.89

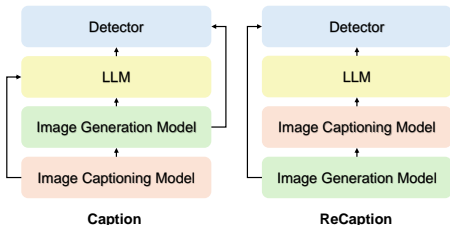


Fig. 5: Comparative overview of the "Caption" and "ReCaption" strategies.

4.8 Qualitative Examples of Synthetic Image-Text-Boxes

Fig. 6 shows qualitative examples of our synthetic image-text-boxes. The first column includes object phrases with specific descriptions (*e.g.* "a Siamese cat"), showcasing our system's ability to produce specific and recognizable entities. The second row presents a complex scenario with a composite subject (*e.g.* "rice beans and meat"). The third column shows a synthetic person while generally depicted with accurate form, exhibits some unrealistic features, suggesting the varying success in capturing human likeness. This finding aligns with the observed improvements on RefCOCO+ Test A (a person-only subset) and indicates that the resolution of object details may not be pivotal for the task of visual grounding. Finally, the fourth column showcases the creative liberties of

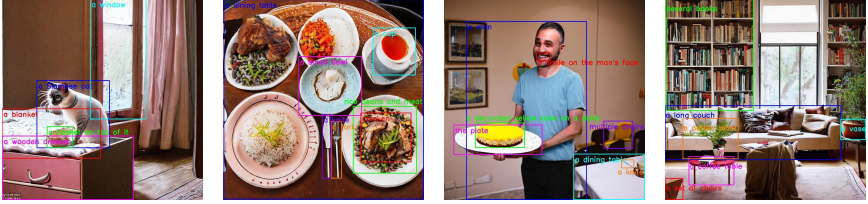


Fig. 6: Qualitative examples of synthetic image-text-boxes. The images are generated by a text-to-image synthesis model. The phrases are generated by an LLM, and the bounding boxes are generated by an object detector model.

the system in generating objects with unusual attributes, such as a coffee table in an unconventional pink color, which shows the diversity in synthetic data. More qualitative examples are presented in the supplementary material.

5 Conclusion

This paper proposes a novel framework that learns from data and models to improve the visual grounding ability of a base vision-and-language model. By leveraging exhaustive image descriptions for image synthesis, utilizing an LLM for phrase extraction, and adopting an open-vocabulary object detector for box synthesis, we demonstrate the efficacy of synthetic image-text-boxes in improving grounding performance. More importantly, integrating the synthetic data with real data yields further performance boosts. Furthermore, we investigate the feasibility of a potentially scalable paradigm at a higher synthetic purity level that relies on LLMs for image description generation.

Limitations and Future Work. While SynGround learns from a suite of powerful large-scale pretrained models, it also inherits their limitations, resulting in certain degradations compared to real data. Future improvements could stem from integrating more advanced models, such as GPT-4 [55] or DALLE-3 [5]. Additionally, this work has not yet explored the integration of layout-conditioned image synthesis models at higher levels of synthetic purity, considering the success and efficiency of SynGround. Although the proposed higher-synthetic purity paradigm empirically shows the capability to generate unlimited data, practical limitations in computational resources limit our ability to generate and train on data at a much larger scale. Future studies should investigate the scaling laws applicable at high-synthetic purity levels.

Broader Impact. Training from synthetic data mitigates privacy issues associated with using real images, since the identities of real individuals are unlikely to be depicted in the data. However, learning from models for visual grounding raises ethical concerns, particularly regarding the amplification of implicit biases in the source data used to train these models we learn from. Such biases may manifest in the oversampling of specific skin colors and genders, such as in certain caption descriptions.

References

1. Abu Alhaija, H., Mustikovela, S.K., Mescheder, L., Geiger, A., Rother, C.: Augmented reality meets computer vision: Efficient data generation for urban driving scenes. *International Journal of Computer Vision* **126**, 961–972 (2018) [4](#)
2. Akbari, H., Karaman, S., Bhargava, S., Chen, B., Vondrick, C., Chang, S.F.: Multi-level multimodal common semantic space for image-phrase grounding. In: *Proceedings of the IEEE/CVF conference on computer vision and pattern recognition*. pp. 12476–12486 (2019) [8](#)
3. Arbelle, A., Doveh, S., Alfassy, A., Shtok, J., Lev, G., Schwartz, E., Kuehne, H., Levi, H.B., Sattigeri, P., Panda, R., et al.: Detector-free weakly supervised grounding by separation. In: *Proceedings of the IEEE/CVF International Conference on Computer Vision*. pp. 1801–1812 (2021) [3](#)
4. Azizi, S., Kornblith, S., Saharia, C., Norouzi, M., Fleet, D.J.: Synthetic data from diffusion models improves imagenet classification. *arXiv preprint arXiv:2304.08466* (2023) [2](#), [4](#)
5. Betker, J., Goh, G., Jing, L., Brooks, T., Wang, J., Li, L., Ouyang, L., Zhuang, J., Lee, J., Guo, Y., et al.: Improving image generation with better captions. *Computer Science*. <https://cdn.openai.com/papers/dall-e-3.pdf> **2**(3), 8 (2023) [14](#)
6. Cascante-Bonilla, P., Shehada, K., Smith, J.S., Doveh, S., Kim, D., Panda, R., Varol, G., Oliva, A., Ordonez, V., Feris, R., et al.: Going beyond nouns with vision & language models using synthetic data. In: *Proceedings of the IEEE/CVF International Conference on Computer Vision*. pp. 20155–20165 (2023) [4](#)
7. Cascante-Bonilla, P., Wu, H., Wang, L., Feris, R.S., Ordonez, V.: Simvqa: Exploring simulated environments for visual question answering. In: *Proceedings of the IEEE/CVF Conference on Computer Vision and Pattern Recognition*. pp. 5056–5066 (2022) [4](#)
8. Changpinyo, S., Sharma, P., Ding, N., Soricut, R.: Conceptual 12m: Pushing web-scale image-text pre-training to recognize long-tail visual concepts. In: *Proceedings of the IEEE/CVF Conference on Computer Vision and Pattern Recognition*. pp. 3558–3568 (2021) [4](#), [7](#)
9. Chen, Y.C., Li, L., Yu, L., El Kholy, A., Ahmed, F., Gan, Z., Cheng, Y., Liu, J.: Uniter: Universal image-text representation learning. In: *European conference on computer vision*. pp. 104–120. Springer (2020) [1](#), [2](#), [3](#)
10. Chen, Y., Li, W., Chen, X., Gool, L.V.: Learning semantic segmentation from synthetic data: A geometrically guided input-output adaptation approach. In: *Proceedings of the IEEE/CVF conference on computer vision and pattern recognition*. pp. 1841–1850 (2019) [4](#)
11. Chiang, W.L., Li, Z., Lin, Z., Sheng, Y., Wu, Z., Zhang, H., Zheng, L., Zhuang, S., Zhuang, Y., Gonzalez, J.E., Stoica, I., Xing, E.P.: Vicuna: An open-source chatbot impressing gpt-4 with 90%* chatgpt quality (March 2023), <https://lmsys.org/blog/2023-03-30-vicuna/> [7](#), [21](#)
12. Dan, Y., Zhao, Y., Li, X., Li, S., Hu, M., Hu, J.: Generative adversarial networks (gan) based efficient sampling of chemical composition space for inverse design of inorganic materials. *npj Computational Materials* **6**(1), 84 (2020) [4](#)
13. Datta, S., Sikka, K., Roy, A., Ahuja, K., Parikh, D., Divakaran, A.: Align2ground: Weakly supervised phrase grounding guided by image-caption alignment. In: *Proceedings of the IEEE/CVF international conference on computer vision*. pp. 2601–2610 (2019) [3](#)

14. Deng, C., Wu, Q., Wu, Q., Hu, F., Lyu, F., Tan, M.: Visual grounding via accumulated attention. In: Proceedings of the IEEE conference on computer vision and pattern recognition. pp. 7746–7755 (2018) [3](#)
15. Deng, J., Yang, Z., Chen, T., Zhou, W., Li, H.: Transvg: End-to-end visual grounding with transformers. In: Proceedings of the IEEE/CVF International Conference on Computer Vision. pp. 1769–1779 (2021) [3](#)
16. Desai, K., Kaul, G., Aysola, Z., Johnson, J.: Redcaps: Web-curated image-text data created by the people, for the people. arXiv preprint arXiv:2111.11431 (2021) [4](#)
17. Dosovitskiy, A., Ros, G., Codevilla, F., Lopez, A., Koltun, V.: Carla: An open urban driving simulator. In: Conference on robot learning. pp. 1–16. PMLR (2017) [4](#)
18. Dou, Z.Y., Peng, N.: Improving pre-trained vision-and-language embeddings for phrase grounding. In: Proceedings of the 2021 Conference on Empirical Methods in Natural Language Processing. pp. 6362–6371 (2021) [2](#), [3](#)
19. Fan, L., Chen, K., Krishnan, D., Katabi, D., Isola, P., Tian, Y.: Scaling laws of synthetic images for model training... for now. arXiv preprint arXiv:2312.04567 (2023) [2](#), [4](#)
20. Gan, C., Schwartz, J., Alter, S., Mrowca, D., Schrimpf, M., Traer, J., De Freitas, J., Kubilius, J., Bhandwaldar, A., Haber, N., et al.: Threedworld: A platform for interactive multi-modal physical simulation. arXiv preprint arXiv:2007.04954 (2020) [4](#)
21. Gomel, E., Shaharbany, T., Wolf, L.: Box-based refinement for weakly supervised and unsupervised localization tasks. In: Proceedings of the IEEE/CVF International Conference on Computer Vision. pp. 16044–16054 (2023) [3](#)
22. Greff, K., Belletti, F., Beyer, L., Doersch, C., Du, Y., Duckworth, D., Fleet, D.J., Gnanaprasasam, D., Golemo, F., Herrmann, C., et al.: Kubric: A scalable dataset generator. In: Proceedings of the IEEE/CVF Conference on Computer Vision and Pattern Recognition. pp. 3749–3761 (2022) [4](#)
23. Gu, X., Lin, T.Y., Kuo, W., Cui, Y.: Open-vocabulary object detection via vision and language knowledge distillation. arXiv preprint arXiv:2104.13921 (2021) [1](#)
24. Gupta, T., Vahdat, A., Chechik, G., Yang, X., Kautz, J., Hoiem, D.: Contrastive learning for weakly supervised phrase grounding. In: European Conference on Computer Vision. pp. 752–768. Springer (2020) [2](#), [3](#)
25. He, K., Gkioxari, G., Dollár, P., Girshick, R.: Mask r-cnn. In: Proceedings of the IEEE international conference on computer vision. pp. 2961–2969 (2017) [3](#)
26. He, R., Sun, S., Yu, X., Xue, C., Zhang, W., Torr, P., Bai, S., Qi, X.: Is synthetic data from generative models ready for image recognition? arXiv preprint arXiv:2210.07574 (2022) [2](#), [4](#)
27. He, R., Cascante-Bonilla, P., Yang, Z., Berg, A.C., Ordonez, V.: Improved visual grounding through self-consistent explanations. arXiv preprint arXiv:2312.04554 (2023) [2](#), [3](#), [4](#), [27](#)
28. He, X., Nassar, I., Kiros, J., Haffari, G., Norouzi, M.: Generate, annotate, and learn: Nlp with synthetic text. Transactions of the Association for Computational Linguistics **10**, 826–842 (2022) [4](#)
29. Inoue, N., Kikuchi, K., Simo-Serra, E., Otani, M., Yamaguchi, K.: Layoutdm: Discrete diffusion model for controllable layout generation. In: Proceedings of the IEEE/CVF Conference on Computer Vision and Pattern Recognition. pp. 10167–10176 (2023) [11](#)
30. Jia, C., Yang, Y., Xia, Y., Chen, Y.T., Parekh, Z., Pham, H., Le, Q., Sung, Y.H., Li, Z., Duerig, T.: Scaling up visual and vision-language representation learning

- with noisy text supervision. In: International conference on machine learning. pp. 4904–4916. PMLR (2021) [1](#)
31. Kamath, A., Singh, M., LeCun, Y., Synnaeve, G., Misra, I., Carion, N.: Mdetrmotulated detection for end-to-end multi-modal understanding. In: Proceedings of the IEEE/CVF International Conference on Computer Vision. pp. 1780–1790 (2021) [2](#)
 32. Kamath, A., Singh, M., LeCun, Y., Synnaeve, G., Misra, I., Carion, N.: Mdetrmotulated detection for end-to-end multi-modal understanding. In: Proceedings of the IEEE/CVF International Conference on Computer Vision. pp. 1780–1790 (2021) [3](#)
 33. Kikuchi, K., Simo-Serra, E., Otani, M., Yamaguchi, K.: Constrained graphic layout generation via latent optimization. In: Proceedings of the 29th ACM International Conference on Multimedia. pp. 88–96 (2021) [11](#)
 34. Kim, D., Wang, K., Saenko, K., Betke, M., Sclaroff, S.: A unified framework for domain adaptive pose estimation. In: European Conference on Computer Vision. pp. 603–620. Springer (2022) [4](#)
 35. Kingma, D.P., Ba, J.: Adam: A method for stochastic optimization. arXiv preprint arXiv:1412.6980 (2014) [8](#)
 36. Krishna, R., Zhu, Y., Groth, O., Johnson, J., Hata, K., Kravitz, J., Chen, S., Kalantidis, Y., Li, L.J., Shamma, D.A., et al.: Visual genome: Connecting language and vision using crowdsourced dense image annotations. International journal of computer vision **123**, 32–73 (2017) [3](#), [7](#), [21](#), [26](#)
 37. Kumar, V., Choudhary, A., Cho, E.: Data augmentation using pre-trained transformer models. arXiv preprint arXiv:2003.02245 (2020) [4](#)
 38. Li, J., Li, D., Savarese, S., Hoi, S.: Blip-2: Bootstrapping language-image pre-training with frozen image encoders and large language models. arXiv preprint arXiv:2301.12597 (2023) [7](#), [9](#), [25](#)
 39. Li, J., Li, D., Xiong, C., Hoi, S.: Blip: Bootstrapping language-image pre-training for unified vision-language understanding and generation. In: International conference on machine learning. pp. 12888–12900. PMLR (2022) [25](#)
 40. Li, J., Selvaraju, R., Gotmare, A., Joty, S., Xiong, C., Hoi, S.C.H.: Align before fuse: Vision and language representation learning with momentum distillation. Advances in neural information processing systems **34**, 9694–9705 (2021) [1](#), [4](#), [5](#), [7](#), [8](#), [12](#), [22](#), [25](#), [27](#)
 41. Li, L.H., Yatskar, M., Yin, D., Hsieh, C.J., Chang, K.W.: Visualbert: A simple and performant baseline for vision and language. arXiv preprint arXiv:1908.03557 (2019) [1](#)
 42. Li, L.H., Zhang, P., Zhang, H., Yang, J., Li, C., Zhong, Y., Wang, L., Yuan, L., Zhang, L., Hwang, J.N., et al.: Grounded language-image pre-training. In: Proceedings of the IEEE/CVF Conference on Computer Vision and Pattern Recognition. pp. 10965–10975 (2022) [1](#), [4](#), [7](#), [10](#)
 43. Li, L.H., Zhang, P., Zhang, H., Yang, J., Li, C., Zhong, Y., Wang, L., Yuan, L., Zhang, L., Hwang, J.N., et al.: Grounded language-image pre-training. In: Proceedings of the IEEE/CVF Conference on Computer Vision and Pattern Recognition. pp. 10965–10975 (2022) [2](#), [26](#)
 44. Li, Y., Liu, H., Wu, Q., Mu, F., Yang, J., Gao, J., Li, C., Lee, Y.J.: Gligen: Open-set grounded text-to-image generation. In: Proceedings of the IEEE/CVF Conference on Computer Vision and Pattern Recognition. pp. 22511–22521 (2023) [10](#)
 45. Lin, T.Y., Maire, M., Belongie, S., Hays, J., Perona, P., Ramanan, D., Dollár, P., Zitnick, C.L.: Microsoft coco: Common objects in context. In: Computer Vision–

- ECCV 2014: 13th European Conference, Zurich, Switzerland, September 6-12, 2014, Proceedings, Part V 13. pp. 740–755. Springer (2014) **7**
46. Liu, H., Li, C., Wu, Q., Lee, Y.J.: Visual instruction tuning. *Advances in neural information processing systems* **36** (2024) **7, 9, 21**
 47. Lu, J., Batra, D., Parikh, D., Lee, S.: Vilbert: Pretraining task-agnostic visiolinguistic representations for vision-and-language tasks. *Advances in neural information processing systems* **32** (2019) **1**
 48. Lu, J., Goswami, V., Rohrbach, M., Parikh, D., Lee, S.: 12-in-1: Multi-task vision and language representation learning. In: *Proceedings of the IEEE/CVF conference on computer vision and pattern recognition*. pp. 10437–10446 (2020) **3**
 49. de Melo, C.M., Torralba, A., Guibas, L., DiCarlo, J., Chellappa, R., Hodgins, J.: Next-generation deep learning based on simulators and synthetic data. *Trends in cognitive sciences* (2022) **4**
 50. Meng, Y., Huang, J., Zhang, Y., Han, J.: Generating training data with language models: Towards zero-shot language understanding. *Advances in Neural Information Processing Systems* **35**, 462–477 (2022) **4**
 51. Mimura, M., Ueno, S., Inaguma, H., Sakai, S., Kawahara, T.: Leveraging sequence-to-sequence speech synthesis for enhancing acoustic-to-word speech recognition. In: *2018 IEEE Spoken Language Technology Workshop (SLT)*. pp. 477–484. IEEE (2018) **4**
 52. Mishra, S., Panda, R., Phoo, C.P., Chen, C.F.R., Karlinsky, L., Saenko, K., Saligrama, V., Feris, R.S.: Task2sim: Towards effective pre-training and transfer from synthetic data. In: *Proceedings of the IEEE/CVF Conference on Computer Vision and Pattern Recognition*. pp. 9194–9204 (2022) **4**
 53. Moreau, A., Piasco, N., Tsishkou, D., Stanciulescu, B., de La Fortelle, A.: Lens: Localization enhanced by nerf synthesis. In: *Conference on Robot Learning*. pp. 1347–1356. PMLR (2022) **4**
 54. Nichol, A., Dhariwal, P., Ramesh, A., Shyam, P., Mishkin, P., McGrew, B., Sutskever, I., Chen, M.: Glide: Towards photorealistic image generation and editing with text-guided diffusion models. *arXiv preprint arXiv:2112.10741* (2021) **4**
 55. OpenAI: Gpt-4 technical report. *ArXiv abs/2303.08774* (2023), <https://api.semanticscholar.org/CorpusID:257532815> **14**
 56. Ordonez, V., Kulkarni, G., Berg, T.: Im2text: Describing images using 1 million captioned photographs. *Advances in neural information processing systems* **24** (2011) **7**
 57. Peng, X., Sun, B., Ali, K., Saenko, K.: Learning deep object detectors from 3d models. In: *Proceedings of the IEEE international conference on computer vision*. pp. 1278–1286 (2015) **4**
 58. Peng, X., Usman, B., Kaushik, N., Hoffman, J., Wang, D., Saenko, K.: Visda: The visual domain adaptation challenge. *arXiv preprint arXiv:1710.06924* (2017) **4**
 59. Plummer, B.A., Wang, L., Cervantes, C.M., Caicedo, J.C., Hockenmaier, J., Lazebnik, S.: Flickr30k entities: Collecting region-to-phrase correspondences for richer image-to-sentence models. In: *Proceedings of the IEEE international conference on computer vision*. pp. 2641–2649 (2015) **8, 27, 28**
 60. Radford, A., Kim, J.W., Hallacy, C., Ramesh, A., Goh, G., Agarwal, S., Sastry, G., Askell, A., Mishkin, P., Clark, J., et al.: Learning transferable visual models from natural language supervision. In: *International conference on machine learning*. pp. 8748–8763. PMLR (2021) **1, 4, 6, 10**
 61. Reimers, N., Gurevych, I.: Sentence-bert: Sentence embeddings using siamese bert-networks. *arXiv preprint arXiv:1908.10084* (2019) **24, 25**

62. Ren, S., He, K., Girshick, R., Sun, J.: Faster r-cnn: Towards real-time object detection with region proposal networks. *Advances in neural information processing systems* **28** (2015) [3](#)
63. Richter, S.R., Vineet, V., Roth, S., Koltun, V.: Playing for data: Ground truth from computer games. In: *Computer Vision—ECCV 2016: 14th European Conference, Amsterdam, The Netherlands, October 11–14, 2016, Proceedings, Part II* 14. pp. 102–118. Springer (2016) [4](#)
64. Rombach, R., Blattmann, A., Lorenz, D., Esser, P., Ommer, B.: High-resolution image synthesis with latent diffusion models. In: *Proceedings of the IEEE/CVF conference on computer vision and pattern recognition*. pp. 10684–10695 (2022) [7](#)
65. Ros, G., Sellart, L., Materzynska, J., Vazquez, D., Lopez, A.M.: The synthia dataset: A large collection of synthetic images for semantic segmentation of urban scenes. In: *Proceedings of the IEEE conference on computer vision and pattern recognition*. pp. 3234–3243 (2016) [4](#)
66. Rosenberg, A., Zhang, Y., Ramabhadran, B., Jia, Y., Moreno, P., Wu, Y., Wu, Z.: Speech recognition with augmented synthesized speech. In: *2019 IEEE automatic speech recognition and understanding workshop (ASRU)*. pp. 996–1002. IEEE (2019) [4](#)
67. Rossenbach, N., Zeyer, A., Schlüter, R., Ney, H.: Generating synthetic audio data for attention-based speech recognition systems. In: *ICASSP 2020–2020 IEEE International Conference on Acoustics, Speech and Signal Processing (ICASSP)*. pp. 7069–7073. IEEE (2020) [4](#)
68. Rozantsev, A., Lepetit, V., Fua, P.: On rendering synthetic images for training an object detector. *Computer Vision and Image Understanding* **137**, 24–37 (2015) [4](#)
69. Russakovsky, O., Deng, J., Su, H., Krause, J., Satheesh, S., Ma, S., Huang, Z., Karpathy, A., Khosla, A., Bernstein, M., et al.: Imagenet large scale visual recognition challenge. *International journal of computer vision* **115**, 211–252 (2015) [4](#), [7](#)
70. Saharia, C., Chan, W., Saxena, S., Li, L., Whang, J., Denton, E.L., Ghasemipour, K., Gontijo Lopes, R., Karagol Ayan, B., Salimans, T., et al.: Photorealistic text-to-image diffusion models with deep language understanding. *Advances in Neural Information Processing Systems* **35**, 36479–36494 (2022) [4](#)
71. Sariyildiz, M.B., Alahari, K., Larlus, D., Kalantidis, Y.: Fake it till you make it: Learning transferable representations from synthetic imagenet clones. In: *CVPR 2023—IEEE/CVF Conference on Computer Vision and Pattern Recognition (2023)* [2](#)
72. Selvaraju, R.R., Cogswell, M., Das, A., Vedantam, R., Parikh, D., Batra, D.: Grad-cam: Visual explanations from deep networks via gradient-based localization. In: *Proceedings of the IEEE international conference on computer vision*. pp. 618–626 (2017) [1](#), [4](#), [7](#)
73. Shaharabany, T., Tewel, Y., Wolf, L.: What is where by looking: Weakly-supervised open-world phrase-grounding without text inputs. *Advances in Neural Information Processing Systems* **35**, 28222–28237 (2022) [3](#)
74. Shaharabany, T., Wolf, L.: Similarity maps for self-training weakly-supervised phrase grounding. In: *Proceedings of the IEEE/CVF Conference on Computer Vision and Pattern Recognition*. pp. 6925–6934 (2023) [3](#)
75. Sharma, P., Ding, N., Goodman, S., Soricut, R.: Conceptual captions: A cleaned, hypernymed, image alt-text dataset for automatic image captioning. In: *Proceedings of the 56th Annual Meeting of the Association for Computational Linguistics (Volume 1: Long Papers)*. pp. 2556–2565 (2018) [26](#), [27](#)

76. Tian, Y., Fan, L., Chen, K., Katabi, D., Krishnan, D., Isola, P.: Learning vision from models rivals learning vision from data. *arXiv preprint arXiv:2312.17742* (2023) [2](#), [4](#), [21](#)
77. Tian, Y., Fan, L., Isola, P., Chang, H., Krishnan, D.: Stablerep: Synthetic images from text-to-image models make strong visual representation learners. *Advances in Neural Information Processing Systems* **36** (2024) [2](#), [4](#)
78. Tucker, A., Wang, Z., Rotalinti, Y., Myles, P.: Generating high-fidelity synthetic patient data for assessing machine learning healthcare software. *NPJ digital medicine* **3**(1), 1–13 (2020) [4](#)
79. Varol, G., Laptev, I., Schmid, C., Zisserman, A.: Synthetic humans for action recognition from unseen viewpoints. *International Journal of Computer Vision* **129**(7), 2264–2287 (2021) [4](#)
80. Varol, G., Romero, J., Martin, X., Mahmood, N., Black, M.J., Laptev, I., Schmid, C.: Learning from synthetic humans. In: *Proceedings of the IEEE conference on computer vision and pattern recognition*. pp. 109–117 (2017) [4](#)
81. Wang, J., Specia, L.: Phrase localization without paired training examples. In: *Proceedings of the IEEE/CVF International Conference on Computer Vision*. pp. 4663–4672 (2019) [3](#)
82. Xiao, F., Sigal, L., Jae Lee, Y.: Weakly-supervised visual grounding of phrases with linguistic structures. In: *Proceedings of the IEEE Conference on Computer Vision and Pattern Recognition*. pp. 5945–5954 (2017) [4](#)
83. Yang, Y., Malaviya, C., Fernandez, J., Swayamdipta, S., Bras, R.L., Wang, J.P., Bhagavatula, C., Choi, Y., Downey, D.: Generative data augmentation for commonsense reasoning. *arXiv preprint arXiv:2004.11546* (2020) [4](#)
84. Yang, Z., Kafle, K., Deroncourt, F., Ordonez, V.: Improving visual grounding by encouraging consistent gradient-based explanations. In: *Proceedings of the IEEE/CVF Conference on Computer Vision and Pattern Recognition*. pp. 19165–19174 (2023) [2](#), [3](#), [4](#), [5](#), [8](#), [12](#), [22](#), [27](#)
85. Yen-Chen, L., Florence, P., Barron, J.T., Lin, T.Y., Rodriguez, A., Isola, P.: Nerf-supervision: Learning dense object descriptors from neural radiance fields. In: *2022 International Conference on Robotics and Automation (ICRA)*. pp. 6496–6503. IEEE (2022) [4](#)
86. Yu, L., Poirson, P., Yang, S., Berg, A.C., Berg, T.L.: Modeling context in referring expressions. In: *Computer Vision–ECCV 2016: 14th European Conference, Amsterdam, The Netherlands, October 11–14, 2016, Proceedings, Part II 14*. pp. 69–85. Springer (2016) [8](#), [27](#), [28](#)
87. Zareian, A., Rosa, K.D., Hu, D.H., Chang, S.F.: Open-vocabulary object detection using captions. In: *Proceedings of the IEEE/CVF Conference on Computer Vision and Pattern Recognition*. pp. 14393–14402 (2021) [1](#)
88. Zheng, J., Zhang, J., Li, J., Tang, R., Gao, S., Zhou, Z.: Structured3d: A large photo-realistic dataset for structured 3d modeling. In: *Computer Vision–ECCV 2020: 16th European Conference, Glasgow, UK, August 23–28, 2020, Proceedings, Part IX 16*. pp. 519–535. Springer (2020) [4](#)

In this section, we provide additional implementation details in Section A, justification of base model selection in Section B, analysis of synthetic text in Section C, comparisons between our synthetic data and web-crawled data in Section D, performance trend across different scales of synthetic data in Section E, and more qualitative examples in Section F.

A Implementation Details

This section presents implementation details, including concept list sampling, as well as LLM prompts used for generating image descriptions, summarizing captions, and extracting text phrases.

A.1 Concept2Text: Concept List and In-Context Examples

Following previous work [76], we assume access to a list of concepts and their distribution in real text T^R (captions from the VG dataset [36]). The concept list curation involves tokenizing the real text T^R and identifying nouns by their part-of-speech (POS) tags. To ensure keeping the relevant information provided in a query for image description generation, we exclude a predefined set of nouns commonly used in prompts or spatial positions: "scene", "scenery", "view", "picture", "image", "photo", "left", "right", "back", "front", "top", "bottom", "middle", "center", "side", "background", "frontmost", "leftmost", "rightmost".

We sample two concepts per query for each image description generation by their frequency in real text T^R . As shown in Fig. 7, an in-context learning example consists of a two-noun query ("Q") and an image description ("A"). The image descriptions are generated by an image captioning model [46] on 500 randomly sampled real images I^R . Then we use POS to randomly extract two nouns as their query. The *Caption2Text* image description generation uses four random in-context learning examples with a random two-noun query.

A.2 Text2Text: LLM Summary

In the *Text2Text* strategy, we prompt an LLM [11] to condense the potentially redundant VG captions T^R for the same image I^R into a summarized version. We include four examples in our prompts, as detailed in Fig. 8. Note that, for each query "Q" and expected answer "A", all orange rows correspond to images generated using the captions from the VG dataset ("Q"); as a counterpart, the yellow rows show images generated by the summarized captions ("A"). Compared to directly concatenating all VG captions, the images generated for summary tend to include more salient objects in the prompts (e.g. surfboards in the 2nd row and the girl in the 4th row), enrich the contextual details (e.g. poles in the 6th row), and remain effective for originally concise captions (e.g. the window and wall in the 8th row).

Q: ["cup", "table"]

A: ["The image showcases a wooden dining table with various food items and tableware arranged on it. A teapot is positioned on the table, along with a kettle and a **cup**. Three donuts are also present on the **table**, with one donut placed near the center, another on the left side, and the third on the right side."]

Q: ["couch", "video"]

A: ["In the image, there are two people playing a **video** game together. A woman is focused on the game, holding a video game remote in her hand, while a man stands behind her, watching her play. There is also a **couch** in the room, providing a comfortable seating area for the two individuals. Additionally, there is a clock on the wall."]

Q: ["trees", "clock"]

A: ["The image features a tall, multi-story building with a prominent **clock** tower at the top. The clock is large and can be seen in the center of the tower. The building is surrounded by **trees** and has a large clock on one of its sides, visible towards the left side of the structure. The overall scene showcases a clock tower that stands out among the surrounding environment."]

Q: ["chair", "vase"]

A: ["The image features a clean, well-furnished apartment with two couches, a **chair**, and a coffee table. The living room area is bright and open, and a large window allows natural light to fill the space. On the coffee table, there is a **vase** with a potted plant, and a book is placed on one of the couches."]

Q: ["cars", "trucks"]

A: ["In this scene, a group of people is gathered at a busy street corner with several vehicles, including **cars** and **trucks**, surrounding the area. There are multiple police cars parked on the side of the street, as well as other cars and trucks scattered throughout the scene. Two people are holding cell phones, likely communicating with others or checking for updates."]

Fig. 7: Random examples from the in-context learning database. The query "Q" contains two nouns, while the expected answer "A" is a crafted image description incorporating the queried nouns.

A.3 Image2Text and Concept2Text: Text Phrase Extraction

Unlike image descriptions obtained from *Concatenation* or *Text2Text* strategies, which consist of a list of phrases, the variants in *Image2Text* and *Concept2Text* are expressed as paragraphs. Due to the ineffectiveness of the “period” or “comma” segment (refer to Table. 2 in the main paper), we experimented with partitioning the sentences by phrase extraction through an LLM. We randomly sample four sentences (*i.e.* segmented by “period”) and extract phrases manually as in-context examples. Fig. 9 presents examples of shorter phrases, while Fig. 10 shows examples of longer phrases.

B Selection of Base Model

We select ALBEF [40] as our base model due to its reported off-the-shelf visual grounding performance and success in further improvement with an attention mask consistency objective [84]. Table 7 provides pointing game accuracy comparisons of two other off-the-shelf vision-and-language models, with ALBEF outperforming other models by a large margin.

C Synthetic Text Analysis

This section supplements the analysis of the factors causing the performance gap with the real data in Section 4.6 of the main paper. Specifically, here we focus



Fig. 8: LLM prompts that summarizes real captions in *Text2Text* strategy. Each example comprises a query "Q" in orange and its expected answer "A" in yellow. "Q" is concatenated real text for an image, and "A" is our crafted summary.

Q: ["there are several cars parked on the street, one of which is a red car near the crosswalk"]
 A: ["several cars", "the street", "a red car", "the crosswalk"]
 Q: ["on the countertop, there is a white plate and a bowl, two cups, a spoon, and a bottle"]
 A: ["the countertop", "a white plate", "a bowl", "two cups", "a spoon", "a bottle"]
 Q: ["the image features a cluttered home office desk with a variety of objects"]
 A: ["a cluttered home office desk", "a variety of objects on the desk"]
 Q: ["a computer monitor is situated towards the left side of the desk, accompanied by a keyboard and a mouse placed directly in front of it"]
 A: ["a computer monitor", "the left side of the desk", "a keyboard", "a mouse"]

Fig. 9: LLM prompts for shorter text phrase T extraction. "Q" is the example query sentence, and "A" is the expected shorter phrase output.

Q: ["there are several cars parked on the street, one of which is a red car near the crosswalk"]
 A: ["there are several cars parked on the street", "a red car near the crosswalk"]
 Q: ["on the countertop, there is a white plate and a bowl, two cups, a spoon, and a bottle"]
 A: ["a white plate on the countertop", "a bowl on the countertop", "two cups on the countertop", "a spoon on the countertop", "a bottle on the countertop"]
 Q: ["the image features a cluttered home office desk with a variety of objects"]
 A: ["a cluttered home office desk", "a variety of objects on the office desk"]
 Q: ["a computer monitor is situated towards the left side of the desk, accompanied by a keyboard and a mouse placed directly in front of it"]
 A: ["a computer monitor is situated towards the left side of the desk", "a keyboard and a mouse placed directly in front of the monitor"]

Fig. 10: LLM prompts for longer text phrase T extraction. "Q" is the example query sentence, and "A" is the expected longer phrase output.

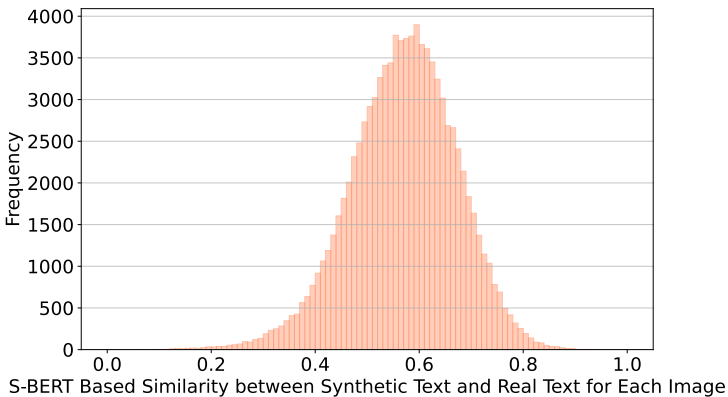
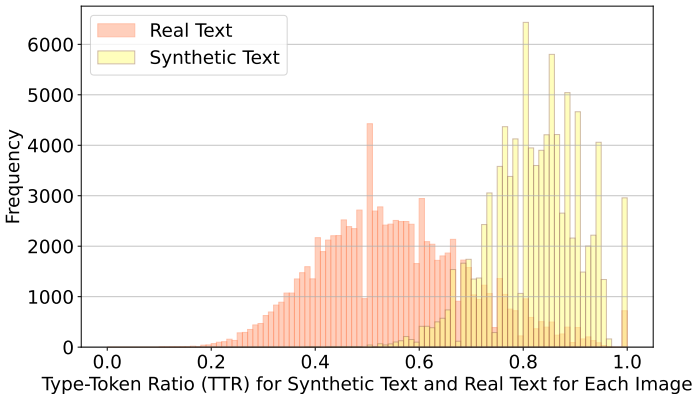


Fig. 11: Distribution of image-wise average Sentence-BERT [61] based cosine similarity between synthetic and real text.

Table 7: Comparisons of off-the-shelf visual grounding performance with pointing game accuracy.

Method	RefCOCO+		Flickr30k
	Test A	Test B	
BLIP-2 [38]	50.09	42.26	64.86
BLIP [39]	61.23	41.07	60.56
ALBEF [40]	69.35	53.77	79.38

**Fig. 12:** Distribution of image-wise type-token ratio for synthetic and real text.

on analyzing the similarity, diversity, and coverage of synthetic text T and real text T^R .

To compute the text similarity, we adopt a pretrained Sentence-BERT [61] to encode text into embeddings. Cosine similarity is then calculated between the embeddings of synthetic and real text corresponding to each image. We determine the text similarity for each synthetic caption by selecting the highest similarity among the real text embeddings, and then track the average similarity for each image. The distribution of the average similarity between synthetic and real text for each image is depicted in Fig. 11, where the highest frequency shows a score of around 0.6. The dissimilarity between the synthetic and real text aligns with the observation of degradation from text synthesis compared to real text (Table 5, main paper).

To delve deeper into the distinctions between synthetic and real texts, we compare their text diversity and coverage. Text diversity is measured using the Type-Token Ratio (TTR), which calculates the ratio of unique token types to the total number of tokens in a text. As shown in Fig. 12, our synthetic text T generally has greater diversity than the real text T^R from VG, indicating more

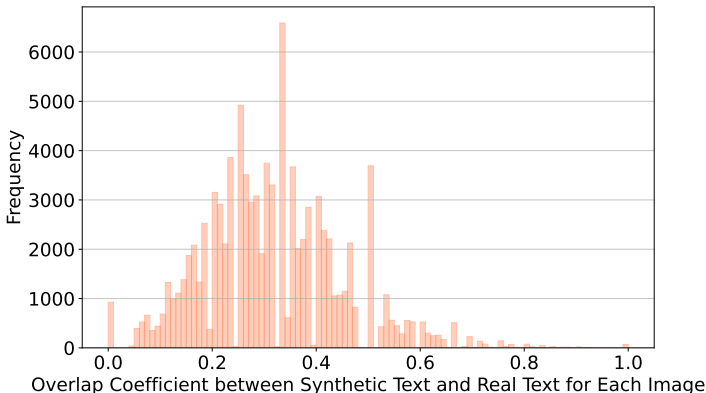


Fig. 13: Distribution of image-wise overlap coefficient between synthetic and real text.

elaborate descriptions that, however, may risk including irrelevant words to the visual content. Additionally, we calculate the overlap coefficient between the unique words in synthetic and real text, assessing the coverage and intersection of vocabulary, peaking at around 0.3 (See Fig. 13). This relatively low coefficient reveals the difference in word usage or content focus between the synthetic text T and the real text T^R .

The observation of a higher TTR in synthetic texts T with a modest overlap coefficient with real texts T^R suggests a trade-off for synthesizing more effective texts for visual grounding. Although the broader vocabulary in synthetic texts T suggests richer and more diverse word usage as well as lower repetition when describing an image, the low overlap score implies a divergence from human-annotated content. Moreover, the presence of approximately 600K fewer texts in the synthetic data may indicate that paraphrasing in real data plays a crucial role.

D Synthetic Data vs. Web-Crawled Data

To showcase the challenge and necessity of generating effective synthetic data tailored for visual grounding, Table 8 presents comparisons of our synthetic data and web-crawled data. The first row is the off-the-shelf performance of our base model, and the second row is its performance after tuning on real Visual Genome data [36]. For fair comparisons, we randomly sample 1M web-crawled data from Conceptual Captions (CC) [75], approximately matching the scale of our synthetic data. As data derived from CC only encompasses images and texts, we add synthetic boxes on top of it from an open-vocabulary detector [43], which is the same box synthesis strategy in our method. Tuning the base model on it achieves (row 3) a 1.82% average performance gain. Additionally, experiments

Table 8: Comparisons of our synthetic data with web-crawled data. The first row is the off-the-shelf base model performance, and the second is the performance after tuning on real data. The third row ("CC") tunes the base model on a subset of CC [75] image-text pairs with generated synthetic boxes, while "CC_{Phrase}" further processes the text through LLM phrase extraction. SynGround_M^H and SynGround_M refer to tuning on our synthetic data, relying on less or more on the real data during synthesis, respectively.

Method	Data	Num.	RefCOCO+		Flickr30k	Δ_{avg}
			Test A	Test B		
ALBEF [40]	-	-	69.35	53.77	79.38	-
AMC [84]	Real	1,649,546	78.89	61.16	86.46	+8.00
CC	Web-Crawled	1,000,000	69.05	54.96	83.94	+1.82
CC _{Phrase}	Web-Crawled	1,000,000	70.35	55.31	85.43	+2.86
SynGround _M ^H	Synthetic	979,861	72.18	55.92	86.30	+3.97
SynGround _M	Synthetic	998,406	73.70	56.35	86.89	+4.81

in Table 2 of the main paper and other work [27] find that the visual grounding ability can be enhanced more significantly with object-centric short phrases rather than generic image descriptions. Considering the text in CC might describe the entire scenario, we further apply our LLM phrase extraction (row 4) and generate synthetic boxes for the synthetic text phrases, leading to a greater average improvement of 2.86%. However, to our best effort, we can not make the web-crawled data reach a similar enhancement with our synthetic data (SynGround_M^H, SynGround_M). Our experimental results indicate that it is non-trivial to curate or synthesize image-text-boxes for visual grounding. The image and text favored by visual grounding seem to have specific properties, such as images with multiple objects and text for region descriptions.

E Trend of Scaling Up

This section explores the potential for scaling synthetic data. Given the limited computation resources to synthesize data and tune a base model, we adopt a downsampling strategy to assess the scaling-up ability of our synthetic data. Specifically, we randomly sample subsets of 25%, 50%, and 75% from our synthetic data, and perform 3 times for each scale to reduce randomness. Fig. 14 illustrates the average pointing game accuracy improvement across RefCOCO+ [86] and Flickr30k [59] benchmarks. We plot the mean improvement at each scale with lines and their standard deviation with shadows. The observed upward trend indicates a promising scaling-up ability of our synthetic data.

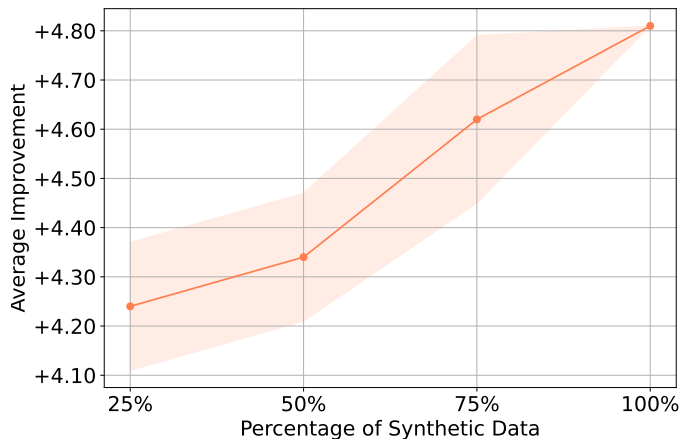


Fig. 14: Average pointing game accuracy improvement on RefCOCO+ [86] and Flickr30k [59] benchmarks at various scales of synthetic data. The line denotes the mean improvement across 3 sampled subsets at each data scale, and the shadow is their standard deviation.

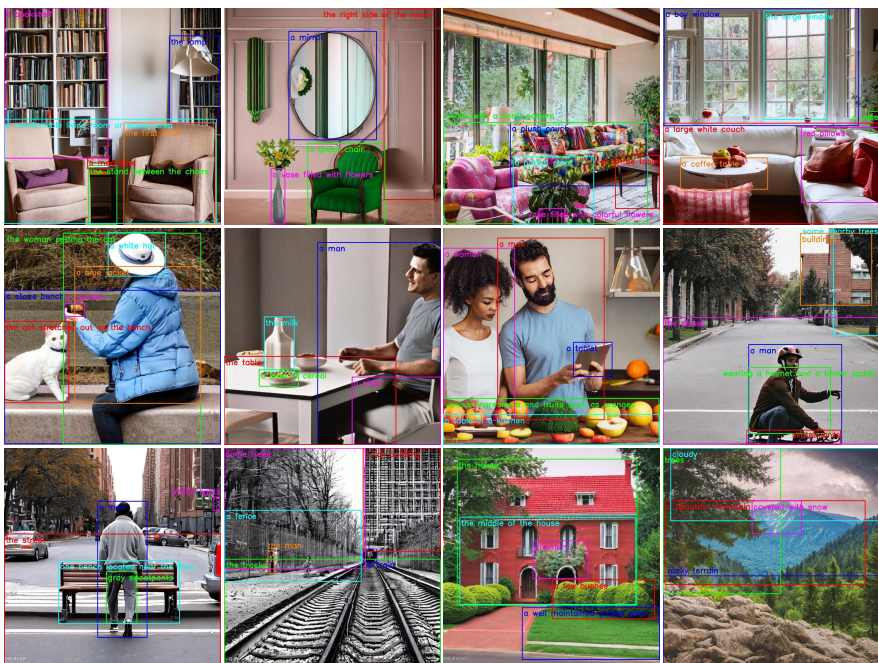


Fig. 15: Qualitative examples of our synthetic image-text-boxes. The images are synthesized by a text-to-image generative model. The texts are generated by an LLM, and their corresponding boxes are obtained from an open-vocabulary object detector.

F Qualitative Examples

In this section, we supplement additional qualitative examples of our synthetic image-text-boxes. For better display, we randomly present a text phrase if there are multiple phrases for overlapping boxes ($\text{IoU} \geq 0.95$). The full dataset will be released upon publication.

In Fig. 15, the first row showcases indoor scenes, the second row features human-related scenes, and the third row depicts outdoor scenes. Intriguingly, our synthetic data shows diversity, such as unconventional design (*e.g.* "the lamp") or color (*e.g.* "a green chair", "chairs with a floral pattern", "red pillows") of furniture in the first row. Despite the presence of artifacts, synthetic humans generally have human-like shapes (row 2). Considering the experimental results (refer to Table 1 in the main paper) that tuning on synthetic data improves grounding performance on the RefCOCO+ Test A, a person-only benchmark, the synthetic human with artifacts still benefits visual grounding. The third row presents some challenging scenarios, including small objects (*e.g.*, "traffic lights," "a train"), detailed descriptions (*e.g.*, "a well-maintained grassy yard"), and complex grammatical structures (*e.g.*, "covered with snow"). In Fig. 16, similar properties are also found in synthetic data generated at a higher synthetic purity level (Section 4.5 of the main paper). Overall, synthetic data with artifacts is able to improve visual grounding performance based on our result, but we expect learning from more advanced image-generative models or text-generative models can lead to further enhancement.

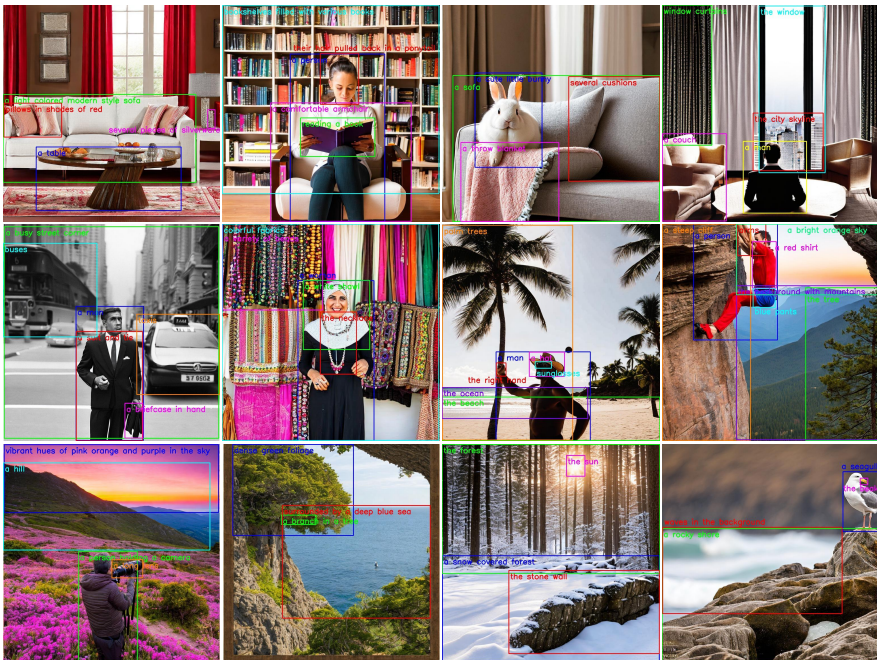


Fig. 16: Qualitative examples of our synthetic image-text-boxes generated at a higher synthetic purity level that relies less on the real data. The images are synthesized according to LLM-generated image descriptions through a text-to-image generative model. The texts are generated by an LLM, and their corresponding boxes are obtained from an open-vocabulary object detector.